THE JOURNAL OF PHYSICAL CHEMISTRY A

Article

Cite This: J. Phys. Chem. A 2019, 123, 3887−3892

pubs.acs.org/JPCA

Using Ionic Liquids To Study the Migration of Semivolatile Organic Vapors in Smog Chamber Experiments

Qing Ye, Ryan C. Sullivan, and Neil M. Donahue*

Center for Atmospheric Particle Studies, Carnegie Mellon University, Pittsburgh, Pennsylvania 15213, United States

ABSTRACT: Atmospheric organic aerosols comprise complex mixtures of a myriad of compounds with a wide range of structures and volatilities. To understand the fate of atmospheric organic aerosols and their contribution to particulate matter pollution, we need to study the relative portion divided between semivolatile organic compounds (SVOCs) and low-volatility organic compounds (LVOCs). SVOCs can effectively migrate and exchange between aerosol populations and thus are more accessible for further reactions and removal processes, while LVOCs will essentially stay in the particle phase. Here, we introduce using ionic liquid droplets as novel sorbents for organic vapors in smog chamber experiments to study the transfer of constituents between aerosol populations and to separate SVOCs and LVOCs from chamber-produced secondary organic aerosols (SOAs). SOA was formed and condensed on the ammonium-sulfate seeds, and later ionic liquid droplets were introduced into the chamber. We show that there are considerable yields of both LVOCs and SVOCs produced from α-pinene ozonolysis, and the uptake of SVOCs into the ionic liquid increases as the amount of reacted α-pinene increases. We also show that the SVOCs absorbed into the ionic liquid re-evaporate more readily compared to SOA originally condensed on the ammonium-sulfate seeds. We are thus able to differentiate the semivolatile components that partition into the extremely polar ionic liquid aerosols from the demonstrably less volatile components also condensed on the ammonium-sulfate seeds. Combined with previous studies using other organic aerosols as solvents to probe SVOC transfer between aerosol populations, we provide a wide set of measurements to probe and constrain the physical and thermodynamic properties of chamber-produced SOA complex.

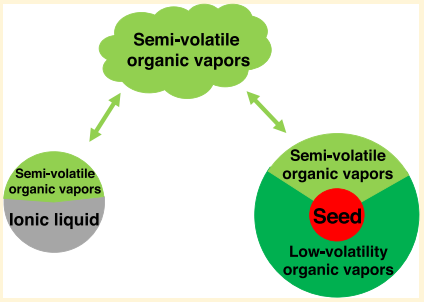

INTRODUCTION

Organic aerosols comprise a major fraction of atmospheric fine particles,[1] which, in turn, are both the largest source of uncertainty[2] in climate forcing and blamed for well over 10% of premature deaths worldwide each year.[3,4] To remain in the condensed phase, organics need an exceptionally low vapor pressure ($p_{vap} \lesssim 10^{-5}$ Pa).[5,6] Because the constituents in organic aerosols are typically also quite reactive in the atmosphere,[7] organic aerosols are often highly oxidized[1] and composed of an enormous number of exotic, highly oxygenated multifunctional molecules.[8] The oxidation chemistry includes recently discovered (for atmospheric chemistry) "autoxidation" of peroxy radicals that can form highly oxygenated organic molecules in a single generation.[9,10] The oxidized organics, in turn, can approach the consistency of pitch,[11] which has called into question whether physical and chemical processes involving diffusion into particles can come to equilibrium over atmospherically relevant timescales.[12]

Multiple experimental techniques have shown that organic aerosols can indeed be highly viscous.[13−18] However, the particles are also tiny, with length scales of an order of 100 nm and complex composition and morphologies that challenge theories suitable for Newtonian fluids such as the Stokes−Einstein relation.[19] Because their formation chemistry is also complex, the characterization of organic aerosols is challenged by coupled unknowns, including composition, reactivity, volatility distribution, diffusivity (also viscosity and physical state), and the activity coefficients of the unknown constituents in different solutions. We have developed a method to constrain many of these properties by combining two separate aerosol populations under conditions where coagulation is negligible and then using single-particle techniques to observe the transfer of constituents between the populations.[20−25] Here, we introduce the use of extremely polar room-temperature ionic liquid (IL) droplets as probe particles to add a highly tunable tool with known physical and thermodynamic properties to probe this complex system. IL droplets also have the advantages of having extremely low vapor pressures and no diffusion limitations—properties may potentially be useful for studying organic aerosols in smog chamber experiments.

MATERIALS AND METHODS

We show the experimental setup and procedure in Scheme 1[20,26] The smog chamber is a 10 m^3 Teflon bag with temperature control, starting at 25 °C in the dark at roughly 5% relative humidity. To produce the "chamber" aerosol population, we first generated 90 nm diameter dry (efflorescent) ammonium-sulfate particles by nebulizing 1 g/L solution and passing the droplets through a diffusion dryer. We injected α-pinene (Sigma-Aldrich, purity of >99%) via a heated septum, followed by a slight excess of ozone to react

Received: March 26, 2019
Published: April 5, 2019

DOI: 10.1021/acs.jpca.9b02847
J. Phys. Chem. A 2019, 123, 3887−3892

Scheme 1. Schematic Diagram for Smog Chamber Experiments Using Ionic Liquid (IL) To Probe SOA Vapor Migration between the Gas and Particle Phase[a]

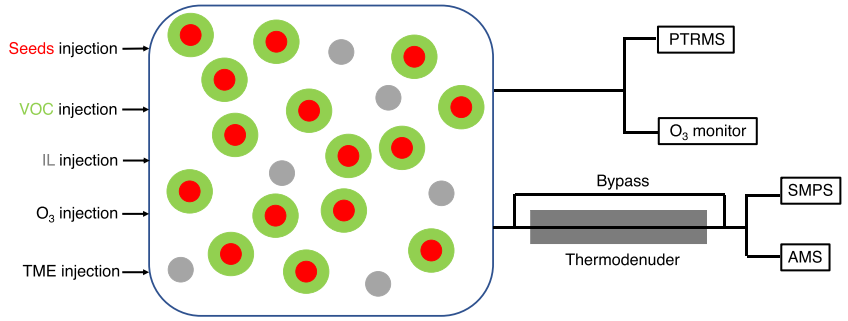

[a]We formed SOA via the reaction of α-pinene and ozone in a temperature-controlled chamber prefilled with dry ammonium-sulfate particles as nonreactive condensation seeds. After the SOA production finished, we injected tetramethylethylene to the chamber to remove residual ozone. Later, we introduced IL droplets into the chamber by atomizing an aqueous solution. We measured gas-phase volatile organic species using a proton transfer reaction-mass spectrometry and particles using an scanning mobility particle sizer (SMPS) and an aerosol mass spectrometer (AMS) with single-particle capability. Upstream of the SMPS and the AMS, particles flowed through either a thermodenuder at various temperatures or through a bypass line at room temperature.

with the α-pinene, producing secondary organic aerosol (SOA) that condensed onto the dry ammonium-sulfate seeds. After this, we injected tetramethylethylene to remove any excess ozone. At this point, the chamber contained an equilibrated aerosol suspension of SOA on the seed particles and vapors in the gas phase; we have previously shown that injecting nonpolar (liquid squalane) "probe" particles into such a suspension results in no detectable mass transfer to the probe particles.[21] To introduce room-temperature ionic liquid probe particles into the chamber, we generated IL droplets by nebulizing 2 g/L solution of 1-ethyl-3-methylimidazolium tetrafluoroborate, $C_6H_{11}BF_4N_2$ (TCI, purity of >97%), followed by a diffusion drier. The ionic liquid particles were on the order of 100 nm in diameter.

We operated a thermodenuder (TD) upstream of an aerosol mass spectrometer (AMS, Aerodyne Inc.) and a scanning mobility particle sizer (SMPS, TSI). The sample flow passed either through the TD, which can heat the particles up to 150 °C, or through a bypass line at room temperature. In the AMS, particles first strike a 600 °C hot surface and then the volatilized molecules are ionized by a 70 eV electron ionization. The resulting ions are separated by a time-of-flight mass spectrometer. The AMS can measure both the aggregated aerosol composition[27] and composition on a single-particle basis by triggering off individual data events (ET) based on user-defined ions on a fast data acquisition card.[25] The trigger setting for the aerosol populations that are originally ionic liquid droplets is m/z 111 $\geq$ 2 ions, as m/z 111 is the dominant mass fragment of the IL we used here in the AMS (more details in the next section). The trigger setting for the aerosol populations that are SOA-coated ammonium-sulfate seeds is m/z 48 (SO^+) $\geq$ 2 ions or m/z 80 (SO_3^+) $\geq$ 2 ions.

RESULTS AND DISCUSSION

Characterization of Ionic Liquid Particle Properties. In Figure 1, we show the aggregated single-particle mass spectra for (a) pure IL particles before they were introduced into the chamber (before mixing), (b) the IL probe particles 2 h after mixing, and (c) the SOA-coated ammonium-sulfate chamber particles 2 h after mixing. The dominant IL fragment, m/z 111, is from the anion ($C_6H_{11}N_2^+$) followed by other important fragments m/z 82 ($C_4H_6N_2^+$) from the anion and m/z 49 (BF_2^+) from the cation. These distinct peaks have minimal overlap with mass fragments from common chemical species such as sulfate and nitrate salts, or from most of the organic fragments in the AMS.[28] To test the selectivity, we set the ET triggering for the ionic liquid (m/z 111 $\geq$ 2 ions) when our chamber contained only SOA-coated ammonium-sulfate particles. The result was an extremely low trigger frequency, indicating that this trigger setting is highly selective to the IL aerosols in our study.

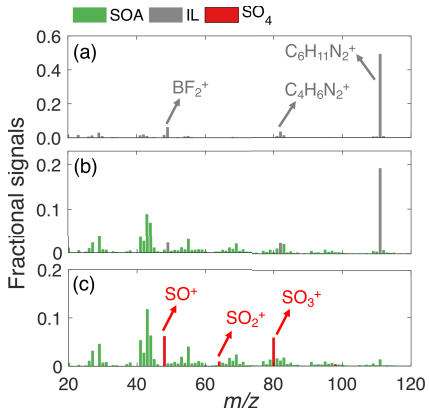

Figure 1. Aggregated particle mass spectra for particles before and after the mixing of chamber and probe particles. (a) Pure IL particles before mixing triggered at the IL fragment m/z 111 ($C_6H_{11}N_2^+$). (b) IL probe particles after being triggered at the IL fragment m/z 111 after injecting into the chamber containing SOA. (c) Chamber particles triggered at the sulfate fragments m/z 48 (SO^+) and m/z 80 (SO_3^+). By triggering at mass fragments with a "tag" in different populations, we are able to separate the two populations.

The ionic liquid particles are essentially nonvolatile. We injected the ionic liquid particles into the chamber and then alternated sampling through the bypass line and the thermodenuder as we systematically raised the thermodenuder temperature up to 120 °C. Figure 2 shows the mass concentration of ionic liquid from the chamber as the thermodenuder temperature increases throughout the experiment. As the figure shows, heating up the particles induces no measurable evaporation. This confirms that ionic liquid particles are effectively nonvolatile and stable up to 120 °C.

DOI: 10.1021/acs.jpca.9b02847
J. Phys. Chem. A 2019, 123, 3887−3892

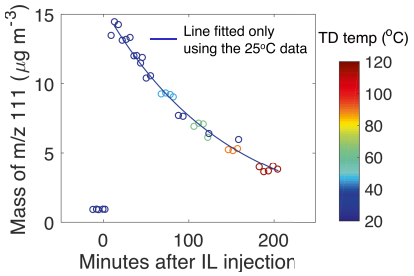

Figure 2. Mass of ionic liquid (IL) fragment m/z 111 at various thermodenuder (TD) temperatures over the course of an experiment. After we injected the IL particles into the chamber, we alternated sampling through the TD or the bypass line while progressively raising the temperature. Data points are color-coded by different temperatures inside the TD as well as the bypass line (which was at a constant 25 °C). The fitted curve is from data points only at the 25 °C, using an exponential function, which reflects the particle wall loss in the chamber. Raising the temperature did not cause the IL particles to evaporate, and all of the data points lie on the room-temperature wall-loss curve, confirming that IL particles are effectively nonvolatile.

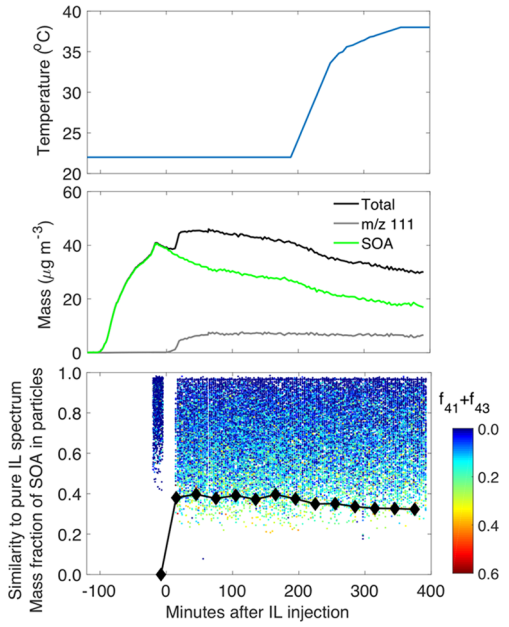

Figure 3. Time series of a typical ionic liquid (IL) SOA mixing experiment. The upper panel shows the temperature of the chamber, the middle panel shows the time series of aggregated bulk mass measurements (without any collection efficiency correction), and the lower panel shows IL probe particles triggered at m/z 111 ≥ 2 ions. The original SOA-coated ammonium-sulfate chamber particles are not shown here. SOA was formed in the chamber at $t < 0$, as shown by the increase of the "SOA" signal in the bulk mass. After the formation stopped, the mass change was dominated by particle wall loss. At $t = 0$, IL particles were introduced into the chamber, denoted by the increase of the dominant fragment in the AMS, m/z 111. The lower panel shows the amount of semivolatile α-pinene SOA material in the IL particles in three ways. Particles shown before $t = 0$ in the lower panel are pure IL as a reference. All particles are color-coded by the fraction of SOA fragments m/z 41 and m/z 43 ($f_{41} + f_{43}$) and plotted on the y-axis according to the cosine similarity of their full mass spectrum to the pure IL particles. The IL spectra are coadded in 30 min intervals and deconvolved against pure IL and pure SOA spectra to determine the SOA fraction plotted on the y-axis with connected black diamonds. Immediately after being added into the chamber, the IL particles absorbed a significant amount of SOA vapors stabilizing at 40% SOA. After heating, the SOA fraction decreased slightly.

We conducted similar tests using pure ammonium-sulfate seeds and we did not see significant evaporation or decomposition up to 110 °C in the TD. We conclude that the ionic liquid particles we used here are effectively as nonvolatile as ammonium-sulfate seeds. Therefore, we do not expect any mass from the ionic liquid particles to exist in the gas phase and consequently there should be no condensation of IL material to any particles. The IL particles function only as a sorbent. This means that, provided coagulation is negligible (as it is under our experimental conditions), if we detect a particle containing ionic liquid mass fragments, we are almost certain that the particle was an ionic liquid particle to start with.

Uptake of Semivolatile Organic Vapors from SOA to Ionic Liquid Particles. After we injected IL probe particles into the chamber in mixing experiments (designated $t = 0$), the chamber contained two particle populations: the chamber population of SOA and the probe population of initially pure IL. Their mass spectra remained distinct. We show a time series of both individual IL particle signals and the bulk mass concentrations in Figure 3. Consistent with our typical protocol, the IL probe particles constituted a relatively small (10−20%) perturbation on the overall chamber conditions. The lower panel of Figure 3 shows the amount of semivolatile SOA absorbed by the IL particles. Individual particles are color-coded by the mass fraction of m/z 41 ($C_3H_5^+$) and m/z 43 ($C_2H_3O^+$), two major fragments from SOA. We also locate each particle on the y-axis according to the cosine similarity score to the ensemble single-particle mass spectrum of pure IL particles. Similarity scores shown before $t < 0$ are from a separate experiment where we measured pure IL droplets and compared individual spectrum with the average IL spectra. We show the similarity scores from pure IL droplets here as a comparison for IL droplets that are exposed to semivolatile organic compounds (SVOCs; $t > 0$). For each of these single-particle measurements, there is significant noise, as the total number of ions per particle is small (typically 3−10 ions per particle). Regardless, after the probe particles enter the chamber, their symbol colors move from consistently dark blue to warmer values and the particles also become substantially less similar to pure bulk IL; this strongly suggests that the IL particles absorb semivolatile organic vapors (SVOCs) from the SOA.

Once we identify the IL particles, we can co-add the mass spectra (here over a 30 min interval) to obtain average spectra. The large black diamonds in Figure 3 are the mass fraction of SOA, f_{SOA}, in the probe particles based on these average spectra. We calculated these using a least-square two-component linear combination of the average spectra from pure IL particles and from pure SOA: $M_{tot} = f_{IL} \cdot M_{IL} + f_{SOA} \cdot M_{SOA} + \mathcal{N}$, where M_{IL} and M_{SOA} are the normalized spectra of IL and SOA, respectively, and $\mathcal{N}$ is noise.

The trend vs time of f_{SOA} in the probe particles indicates that the vapor uptake is swift. Within 30 min (the first aggregated post-injection data point), the IL particles contain 40% SOA, and this does not change for the following 3 h. This is consistent with the absorption of semivolatile SOA constituents into IL droplets that are liquid at room temperature, without any diffusion limitations delaying the

DOI: 10.1021/acs.jpca.9b02847
J. Phys. Chem. A 2019, 123, 3887−3892

equilibration of gas- and particle-phase partitioning. The high mass fraction of SOA in the probe particles also suggests that the equilibrium suspension of SOA produced from α-pinene ozonolysis contains a significant amount of semivolatile vapors ($C^* \gtrsim 1\ \mu g/m^3$), as these vapors will be able to readily migrate between different particle populations within the timescale of these experiments. Less volatile constituents have repartitioning timescales from ~200 nm particles that exceed 10 h.[29] It also indicates a significant thermodynamic driving force for the SVOCs into the IL probe particles when they enter the otherwise equilibrated suspension. The 40% asymptotic mass fraction of SOA in the IL indicates a (mass-based) activity of 0.4 for the SVOCs in the IL if the SOA−IL system were an ideal solution; given the high polarity of the IL, the actual SVOC activity is likely to be substantially higher.

After about 3 h, we raised the chamber temperature to 38 °C. After this, both the SOA mass fraction in the probe particles and the bulk SOA mass decreased slightly. This indicates some evaporation of SVOCs from the IL, though the full interpretation is challenging because the SVOCs are in equilibrium with a much larger population of SOA chamber particles. Below, we will describe the behavior of SVOC evaporation from the IL particles using a thermodenuder that covers a much higher temperature range.

We performed several similar experiments with different initial α-pinene concentrations to explore the activity of SOA in IL particles for different SOA loadings. In Figure 4, we show

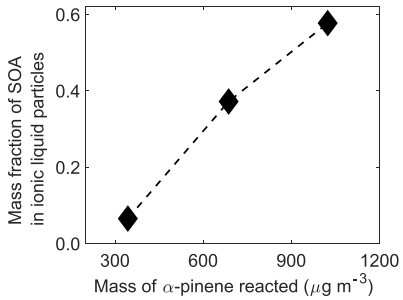

Figure 4. Mass fraction of SOA in IL particles as a function of α-pinene reacted 2 h after they are exposed to an equilibrated SOA aerosol suspension containing SVOCs. Increasing α-pinene reacted results in higher SVOC activity and higher absorption into the IL.

f_{SOA} in the probe particles at t = 2 h plotted against the reacted α-pinene concentration. As the amount of reacted α-pinene increases, the activity of SVOCs in the IL particles increases; more VOC oxidation leads to a larger SVOC saturation ratio. At very high amounts of reacted precursor ($\approx$ 1000 $\mu g/m^3$), the IL particles contain 58% SOA at t = 2 h. Ye et al.[22] used poly(ethylene glycol) (PEG400) to absorb SVOC from α-pinene ozonolysis and found that the activity of SVOC in PEG particles also increases with reacted α-pinene.

The extent of mixing revealed in Figure 4 shows that the aggregate SVOC activity increases with increasing amounts of oxidized α-pinene and also that the activity reaches a high value. However, to quantify the gas-phase activity (saturation ratio) from the condensed-phase mass fraction after mixing, we need to know the activity coefficients. There is every reason to expect relatively high activity coefficients between the modestly polar SOA and the highly polar IL. Gorkowski et al.[30] found that α-pinene SOA particles phase-separate from aqueous sodium chloride droplets levitated using optical tweezers, suggesting finite solubility of α-pinene SOA in polar salt solutions. Ye et al.[31] used Hansen solubility parameters to rationalize the solubility of α-pinene SOA in organic seed particles with varying polarities. This framework can be extended to highly polar systems such as salts but we do not yet have sufficient information regarding the SOA volatility distribution and the detailed molecular composition to estimate the exact solubility of SOA species in the ionic liquid particles. However, these results provide another constraint complementing the literature on the overall activity of SOA from α-pinene in condensed phases of varying polarities.

Evaporation of SVOCs from IL Particles. The mixing experiments described above imply that the α-pinene SOA has a substantial fraction of SVOCs but also that the majority of the SOA (on the dry ammonium-sulfate seeds) is much less volatile, consistent with recent findings regarding autoxidation.[10,32] If the IL probe particles truly contain only the SVOC fraction of the SOA, then the SOA in the probe particles should be more volatile than the SOA originally on the dry ammonium-sulfate chamber particles, even though the SVOCs are presumably mixed into the IL particles, whereas the original SOA, consisting of both low-volatility organic compounds (LVOCs) and SVOCs, is presumably coating the dry ammonium-sulfate seeds as a separate phase. After mixing IL probe particles into a chamber with SOA coating dry ammonium-sulfate particles, there is no way to assess the separate volatility of the two populations using bulk methods. However, the single-particle technique we use directly on the chamber works equally well downstream of a thermodenuder. We explored this thermal volatility during a high-concentration mixing experiment with 366 $\mu g/m^3$ of SOA coating dry ammonium-sulfate seeds.

We sampled particles from the chamber containing the two populations through the thermodenuder and calculated the ratio of SOA to the nonvolatile seeds (dry ammonium sulfate and IL) for each population at each temperature. We then normalized to the room-temperature value to give the mass fraction remaining for each population, as shown in Figure 5.

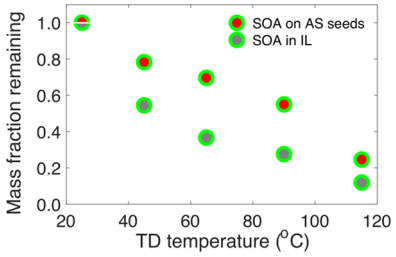

Figure 5. Mass fraction remaining of SOA on dry ammonium-sulfate seeds (AS) and in IL droplets after passing through a thermodenuder (TD). The SOA absorbed in the IL droplets is more volatile than the SOA on the sulfate seeds.

For the IL probe particles, at 45 °C, 40% of the SVOCs evaporated, and at 115 °C, about 90% of the SVOCs evaporated, confirming that the condensation of SVOCs in the IL particles is indeed reversible. Significantly less SOA evaporated from the ammonium-sulfate particles at each temperature, confirming that overall the total SOA contains both a substantial SVOC fraction but also a large LVOC fraction.

Both of these findings are significant. The probe particle method is effective at constraining the semivolatile fraction of

DOI: 10.1021/acs.jpca.9b02847
J. Phys. Chem. A 2019, 123, 3887−3892

an aerosol population, and in this case, there is a significant semivolatile fraction. However, the α-pinene SOA also has a majority low-volatility fraction, even under the high-concentration conditions of a "traditional" smog chamber experiment. Until very recently (and to this day in many chemical transport models), most of the SOA was parameterized as almost entirely semivolatile.[33,34]

CONCLUSIONS

Ionic liquids are fascinating solvents that are effectively nonvolatile, and here we use them in a novel way to generate nanovessels to sorb semivolatile organics in secondary organic aerosols important to atmospheric chemistry. Using single-particle methods, we can numerically unmix these populations to determine the semivolatile fraction in SOA populations. The liquid probe particles allow us to separate simple low-volatility content[10] from postulated kinetic limitations in mass transfer such as high viscosity and thus low diffusivity in SOA particles.[35] Here, an ensemble of effectively nonvolatile liquid probe particles, including various ionic liquids and also polymers such as PEG and methylated PEG,[22] may prove to be effective, also allowing us to separate simple and reversible absorption of semivolatile species from (possibly irreversible) reactive uptake.

AUTHOR INFORMATION

Corresponding Author

*E-mail: nmd@andrew.cmu.edu.

ORCID

Ryan C. Sullivan: 0000-0003-0701-7158

Neil M. Donahue: 0000-0003-3054-2364

Notes

The authors declare no competing financial interest.

ACKNOWLEDGMENTS

This work is supported by the U.S. National Science Foundation under grants MRI—CBET0922643 and CHE—1807530. The authors also want to thank the Faculty for the Future Fellowship from the Schlumberger Foundation.

REFERENCES

(1) Jimenez, J. L.; Canagaratna, M.; Donahue, N.; Prevot, A.; Zhang, Q.; Kroll, J. H.; DeCarlo, P. F.; Allan, J. D.; Coe, H.; Ng, N.; et al. Evolution of organic aerosols in the atmosphere. *Science* **2009**, *326*, 1525−1529.

(2) *Climate Change 2013: The Physical Science Basis, Contribution of Working Groups I to the Fifth Assessment Report of the Intergovernmental Panel on Climate Change*, 2013.

(3) Apte, J. S.; Marshall, J. D.; Cohen, A. J.; Brauer, M. Addressing global mortality from ambient PM2. 5. *Environ. Sci. Technol.* **2015**, *49*, 8057−8066.

(4) Lelieveld, J.; Haines, A.; Pozzer, A. Age-dependent health risk from ambient air pollution: a modelling and data analysis of childhood mortality in middle-income and low-income countries. *Lancet Planet. Health* **2018**, *2*, e292−e300.

(5) Pankow, J. F. An absorption model of the gas/aerosol partitioning involved in the formation of secondary organic aerosol. *Atmos. Environ.* **1994**, *28*, 189−193.

(6) Bilde, M.; Barsanti, K.; Booth, M.; Cappa, C. D.; Donahue, N. M.; Emanuelsson, E. U.; McFiggans, G.; Krieger, U. K.; Marcolli, C.; Topping, D.; et al. Saturation Vapor Pressures and Transition Enthalpies of Low Volatility Organic Molecules of Atmospheric Relevance: From Dicarboxylic Acids to Complex Mixtures. *Chem. Rev.* **2015**, *115*, 4115−4156.

(7) Donahue, N.; Chuang, W.; Epstein, S.; Kroll, J.; Worsnop, D.; Robinson, A.; Adams, P.; Pandis, S. Why do organic aerosols exist? Understanding aerosol lifetimes using the two-dimensional volatility basis set. *Environ. Chem.* **2013**, *10*, 151−157.

(8) Kroll, J. H.; Donahue, N. M.; Jimenez, J. L.; Kessler, S. H.; Canagaratna, M. R.; Wilson, K. R.; Altieri, K. E.; Mazzoleni, L. R.; Wozniak, A. S.; Bluhm, H.; et al. Carbon oxidation state as a metric for describing the chemistry of atmospheric organic aerosol. *Nat. Chem.* **2011**, *3*, 133−139.

(9) Crounse, J. D.; Nielsen, L. B.; Jørgensen, S.; Kjaergaard, H. G.; Wennberg, P. O. Autoxidation of organic compounds in the atmosphere. *J. Phys. Chem. Lett.* **2013**, *4*, 3513−3520.

(10) Ehn, M.; Thornton, J. A.; Kleist, E.; Sipilä, M.; Junninen, H.; Pullinen, I.; Springer, M.; Rubach, F.; Tillmann, R.; Lee, B.; et al. A large source of low-volatility secondary organic aerosol. *Nature* **2014**, *506*, 476−479.

(11) Koop, T.; Bookhold, J.; Shiraiwa, M.; Pöschl, U. Glass transition and phase state of organic compounds: dependency on molecular properties and implications for secondary organic aerosols in the atmosphere. *Phys. Chem. Chem. Phys.* **2011**, *13*, 19238−19255.

(12) Shiraiwa, M.; Ammann, M.; Koop, T.; Pöschl, U. Gas uptake and chemical aging of semisolid organic aerosol particles. *Proc. Natl. Acad. Sci. U.S.A.* **2011**, *108*, 11003−11008.

(13) Virtanen, A.; Joutsensaari, J.; Koop, T.; Kannosto, J.; Yli-Pirilä, P.; Leskinen, J.; Mäkelä, J. M.; Holopainen, J. K.; Pöschl, U.; Kulmala, M.; et al. An amorphous solid state of biogenic secondary organic aerosol particles. *Nature* **2010**, *467*, 824−827.

(14) Renbaum-Wolff, L.; Grayson, J. W.; Bateman, A. P.; Kuwata, M.; Sellier, M.; Murray, B. J.; Shilling, J. E.; Martin, S. T.; Bertram, A. K. Viscosity of α-pinene secondary organic material and implications for particle growth and reactivity. *Proc. Natl. Acad. Sci. U.S.A.* **2013**, *110*, 8014−8019.

(15) Price, H. C.; Mattsson, J.; Zhang, Y.; Bertram, A. K.; Davies, J. F.; Grayson, J. W.; Martin, S. T.; O'Sullivan, D.; Reid, J. P.; Rickards, A. M.; et al. Water diffusion in atmospherically relevant α-pinene secondary organic material. *Chem. Sci.* **2015**, *6*, 4876−4883.

(16) Pajunoja, A.; Lambe, A. T.; Hakala, J.; Rastak, N.; Cummings, M. J.; Brogan, J. F.; Hao, L.; Paramonov, M.; Hong, J.; Prisle, N. L.; et al. Adsorptive uptake of water by semisolid secondary organic aerosols. *Geophys. Res. Lett.* **2015**, *42*, 3063−3068.

(17) Song, M.; Liu, P.; Hanna, S. J.; Zaveri, R. A.; Potter, K.; You, Y.; Martin, S.; Bertram, K. Relative humidity-dependent viscosity of secondary organic material from toluene photo-oxidation and possible implications for organic particulate matter over megacities. *Atmos. Chem. Phys.* **2016**, *16*, 8817−8830.

(18) Marshall, F. H.; Miles, R. E.; Song, Y.-C.; Ohm, P. B.; Power, R. M.; Reid, J. P.; Dutcher, C. S. Diffusion and reactivity in ultraviscous aerosol and the correlation with particle viscosity. *Chem. Sci.* **2016**, *7*, 1298−1308.

(19) Chenyakin, Y.; Ullmann, D. A.; Evoy, E.; Renbaum-Wolff, L.; Kamal, S.; Bertram, A. K. Diffusion coefficients of organic molecules in sucrose-water solutions and comparison with Stokes-Einstein predictions. *Atmos. Chem. Phys.* **2017**, *17*, 2423−2435.

(20) Robinson, E. S.; Saleh, R.; Donahue, N. M. Organic aerosol mixing observed by single-particle mass spectrometry. *J. Phys. Chem. A* **2013**, *117*, 13935−13945.

(21) Robinson, E. S.; Saleh, R.; Donahue, N. M. Probing the evaporation dynamics of mixed SOA/squalane particles using size-resolved composition and single-particle measurements. *Environ. Sci. Technol.* **2015**, *49*, 9724−9732.

(22) Ye, P.; Ding, X.; Ye, Q.; Robinson, E. S.; Donahue, N. M. Uptake of Semi-volatile Secondary Organic Aerosol Formed from α-Pinene into Non-volatile Polyethylene Glycol Probe Particles. *J. Phys. Chem. A* **2015**, *120*, 1459−1467.

(23) Robinson, E. S.; Donahue, N. M.; Ahern, A. T.; Ye, Q.; Lipsky, E. Single-particle measurements of phase partitioning between primary and secondary organic aerosols. *Faraday Discuss.* **2016**, *189*, 31−49.

DOI: 10.1021/acs.jpca.9b02847
J. Phys. Chem. A 2019, 123, 3887−3892

(24) Ye, Q.; Robinson, E. S.; Ding, X.; Ye, P.; Sullivan, R. C.; Donahue, N. M. Mixing of secondary organic aerosols versus relative humidity. *Proc. Natl. Acad. Sci. U.S.A.* **2016**, *113*, 12649−12654.
(25) Ye, Q.; Upshur, M. A.; Robinson, E. S.; Geiger, F. M.; Sullivan, R. C.; Thomson, R. J.; Donahue, N. M. Following particle-particle mixing in atmospheric secondary organic aerosols by using isotopically labeled terpenes. *Chem* **2018**, *4*, 318−333.
(26) Huff Hartz, K. E.; Rosenørn, T.; Ferchak, S. R.; Raymond, T. M.; Bilde, M.; Donahue, N. M.; Pandis, S. N. Cloud condensation nuclei activation of monoterpene and sesquiterpene secondary organic aerosol. *J. Geophys. Res.: Atmos.* **2005**, *110*, DOI: 10.1029/2004JD005754.
(27) DeCarlo, P. F.; Kimmel, J. R.; Trimborn, A.; Northway, M. J.; Jayne, J. T.; Aiken, A. C.; Gonin, M.; Fuhrer, K.; Horvath, T.; Docherty, K. S.; et al. Field-deployable, high-resolution, time-of-flight aerosol mass spectrometer. *Anal. Chem.* **2006**, *78*, 8281−8289.
(28) Allan, J. D.; Delia, A. E.; Coe, H.; Bower, K. N.; Alfarra, M. R.; Jimenez, J. L.; Middlebrook, A. M.; Drewnick, F.; Onasch, T. B.; Canagaratna, M. R.; et al. A generalised method for the extraction of chemically resolved mass spectra from Aerodyne aerosol mass spectrometer data. *J. Aerosol Sci.* **2004**, *35*, 909−922.
(29) Donahue, N. M.; Chuang, W. K.; Schervish, M. *Advances in Chemistry of the Contemporary Atmosphere Chapter Gas-Phase Organic Oxidation Chemistry and Atmospheric Particles*; World Scientific, 2019.
(30) Gorkowski, K.; Donahue, N. M.; Sullivan, R. C. Emulsified and Liquid-Liquid Phase-Separated States of α-Pinene Secondary Organic Aerosol Determined Using Aerosol Optical Tweezers. *Environ. Sci. Technol.* **2017**, *51*, 12154−12163.
(31) Ye, J.; Gordon, C. A.; Chan, A. W. Enhancement in secondary organic aerosol formation in the presence of preexisting organic particle. *Environ. Sci. Technol.* **2016**, *50*, 3572−3579.
(32) Bianchi, F.; Kurtén, T.; Riva, M.; Mohr, C.; Rissanen, M.; Roldin, P.; Berndt, T.; Crounse, J.; Wennberg, P.; Mentel, T. F.; et al. Highly oxygenated molecules (HOM) from gas-phase autoxidation of organic peroxy radicals: A key contributor to atmospheric aerosol. *Chem. Rev.* **2019**, *119*, 3472−3509.
(33) Pun, B. K.; Wu, S.-Y.; Seigneur, C.; Seinfeld, J. H.; Griffin, R. J.; Pandis, S. N. Uncertainties in modeling secondary organic aerosols: Three-dimensional modeling studies in Nashville/Western Tennessee. *Environ. Sci. Technol.* **2003**, *37*, 3647−3661.
(34) Presto, A. A.; Donahue, N. M. Investigation of α-pinene. ozone secondary organic aerosol formation at low total aerosol mass. *Environ. Sci. Technol.* **2006**, *40*, 3536−3543.
(35) Vaden, T. D.; Imre, D.; Beránek, J.; Shrivastava, M.; Zelenyuk, A. Evaporation kinetics and phase of laboratory and ambient secondary organic aerosol. *Proc. Natl. Acad. Sci. U.S.A.* **2011**, *108*, 2190−2195.

DOI: 10.1021/acs.jpca.9b02847
J. Phys. Chem. A 2019, 123, 3887−3892